Wormholes in chemical space connecting torus knot and torus link π-electron density topologies

Henry S. Rzepa

Received 17th June 2008, Accepted 11th November 2008
First published as an Advance Article on the web 13th January 2009
DOI: 10.1039/b810301a

Möbius aromaticities can be considered as deriving from cyclic delocalized π-electron densities $\rho(r)_\pi$ which have the topological form of either a two-component torus link or a single-component torus knot. These two topological forms are distinguished by their (non-zero) linking number L_k, which describes how many times the two components of a torus link cross each other or the single component of a torus knot crosses with itself. The special case of Hückel or benzenoid aromaticity is associated with a π-electron density that takes the form of a two-component torus link for which the linking number is zero. A class of molecule has been identified which here is termed a Janus aromatic, and which bears the characteristics of both a two-component torus link and a single-component torus knot in the topology of the π-electron density. This is achieved by the formation of one (or more) wormholes or throats in the π-electron density connecting the two torus forms, which can impart a Janus-like dual personality to the aromaticity of the system. The impact of such wormholes on the overall π-delocalized aromaticity of such molecules is approximately estimated using a NICS(rcp) index, and subdivides into two types; those where the forms of aromaticity associated with a torus link and a torus knot cooperate and those where they oppose.

Introduction

The Möbius strip is one of the earliest investigated topological classes, and its properties were independently described by both Listing and Möbius in 1858.[1] It was investigated as a chemical concept by Heilbronner more than 100 years later,[2] who invoked it in a theoretical analysis of the π-electronic delocalization of twisted cyclic [N]annulenes. For a further 40 years, attention was concentrated purely on the first member of the class, in which only a single half-twist has been imparted to the π-electronic ribbon or to a nuclear ladder.[3] Recently the focus has extended to ribbons with more than one half twist. These include double-half-twist systems, which have been revealed as adopting a lemniscular (figure-eight)[4] form, and a pentadecamanganese metallacycle identified as exhibiting six half-twists.[5] Whilst Heilbronner's theoretical treatment was purely a two-dimensional one, it has been recognized[6] that a more complete analysis involves a three-dimensional property known as writhe, with an associated need to redefine the precise meaning of the term *twist*. The latter, which can be approximated in a π-electronic annulene as the sum of the local torsion angles γ between adjacent 2p-AOs, is merely one of two components (T_w and W_r), which comprise a more general topological descriptor known as the linking number (eqn (1))[6]

$$L_k = T_w + W_r \quad (1)$$

Significantly, whilst neither T_w nor W_r need be an integer quantity, the linking number must be so (conveniently expressed in units of π for describing π-electronic ribbons). The electron π-density of an annulene can itself be described by another topological geometrical object known as a torus,[6,7] which is formally defined as a surface of revolution generated by revolving a circle in three-dimensional space about an axis coplanar with the circle, and which does not touch the circle. Two forms of the torus curve are of particular relevance to the annulene π-electron density: a single component torus knot and a two-component torus link. The latter is conventionally defined by its linking number L_k, which in this case represents the number of times that each curve winds around the other during a single cycle,[8] and which again for our purposes is most conveniently expressed in (positive or negative and even integer) units of π. For the purpose of comparison with the torus link, the linking number of the single component torus knot making two circuits rather than one to return to the starting point is normalized to a single circuit and its value can again be a positive or negative (but now an odd) integer in units of π (Fig. 1).[9]

We have recently described[6,7] in detail the various relationships between two- and three-dimensional π-electronic 2p-AO basis set ribbons and the description of the resulting LCAO molecular orbitals and related electron density functions. In particular, the π-electron density $\rho(r)_\pi$ of a Möbius annulene as described by an odd linking number (in units of π) takes the form of a torus knot, which involves a double encirclement of the annulene ring (Fig. 1b) and which will exhibit an odd number of crossings of itself during the circuit. A second class consists of those annulenes which sustain an even (or zero) linking number and for which $\rho(r)_\pi$ can be compared to a torus link. This comprises a single encirclement by each of two separate torus components, which will cross each other an

Department of Chemistry, Imperial College London, South Kensington Campus, London, UK SW7 2AY

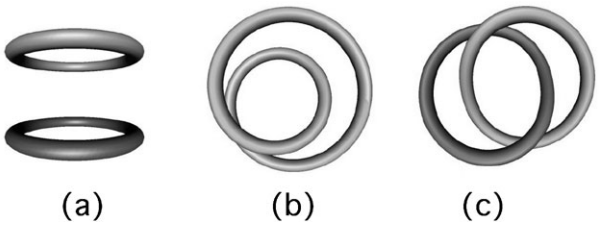

Fig. 1 Schematic illustration of: (a) a 2_0 torus link. If the torus is constructed from an unsigned electron density $\rho(r)$ function, the symmetry elements can include a plane; (b) a 1_1 torus knot which can sustain C_2-symmetry; and (c) a 2_2 torus link which can sustain D_2-symmetry but which has no plane of symmetry. The linking numbers of these torus curves take the values $L_k = 0$, 1 and 2 (in units of π) for respectively (a), (b) and (c). The diagrams were produced using KnotPlot (http://knotplot.com/).

even (or zero) number of times (Fig. 1c or a, respectively). These two types of torus curve therefore have quite different topological properties.

This latter point is pertinent when considering the chiral properties of Möbius-like annulenes.[6] An object having any non-zero value of the L_k must be dis-symmetric (having at best only axes of symmetry); it cannot be superimposed upon its mirror image, and must therefore be capable of existence as an enantiomeric pair, defined by linking numbers of opposite sign ($\pm L_k$). A foremost question when describing chemical enantiomers is what the inter-conversion (enantiomerization) barrier might be and what the nature of the transition state defining this barrier is. Whilst it is possible for two enantiomeric objects to be connected by a continuous path which passes through only chiral configurations (such objects are said to be chirally connected[10]), in the simplest chemical cases such as those considered here, one transition state along the pathway to enantiomerization will not itself be dis-symmetric but will also bear a mirror plane of symmetry in which reflection can occur.[11] One aspect of the topological analysis is that the linking number of the $\rho(r)_\pi$ torus at such a transition state geometry must in fact be zero (Fig. 1a). The issue now is how to convert an object with a π-electronic topology corresponding to a non-zero linking number into one with a zero linking number for the π-wavefunction on a continuous potential energy surface. The integer linking number itself (being an integer) cannot continuously morph from one to the other, and an apparent contradiction results.

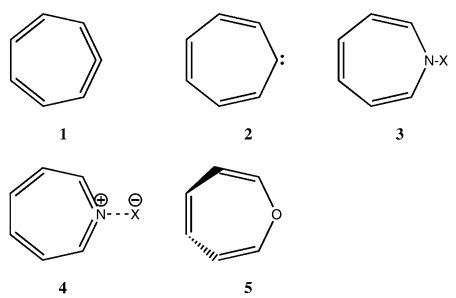

1 2 3 4 5

One of the earliest suggestions for a cyclic neutral annulene that might support (some) Möbius character was the 8-π-electron allene system **1**.[12] Derivatives of this type of ring are known, and the mechanism for enantiomerization[13] of this dis-symmetric ring has been computed as proceeding *via* a planar transition state **2** involving 6-π-electrons, with two erstwhile π-electrons from **1** being converted (sequestered) *via* an in-plane σ-carbene. The potential energy surface is therefore underpinned by a continuous transformation of two π electrons in **1** into two σ-electrons in **2**. More significantly, the topological descriptor of the π-electron component of this transformation involves a Möbius-like torus knot ($L_k = 1$ = odd, *cf.* Fig. 1b) for **1** and a two component torus link ($L_k = 0$ = even, *cf.* Fig. 1a) for **2**. Shortly after this discussion of **1**, the azepine **3** was identified with similar properties.[14] Thus **3** (which sustains a plane of symmetry passing through the N–X group) can be twisted into a C_2-symmetric isomer, for which the valence bond structure **4** can be written, and at which point the ring can be regarded as being iso-electronic with **1**. Both systems exhibit a continuous potential energy surface between the C_2-dis-symmetric and the non-dis-symmetric (C_s symmetric) geometries. Clearly, as **3** distorts along a C_2-symmetric mode, the degree of Möbius character increases from zero to some finite value. A topological interpretation of this process is the subject of this article.

Results and discussion

8-π/6-π-Systems

We have previously demonstrated[7] that the $\rho(r)_\pi$ isosurface of cyclic annulenes takes the form of a torus, and in particular for an (ideal) single half-twist π-Möbius system, it is a torus 1_1 knot with a linking number $L_k = 1$ (*cf.* Fig. 1b). For a planar annulene (for example the enantiomerization transition state **2**) it has the form of a 0_2 torus link (*cf.* Fig. 1a) for which the linking number is precisely zero. A quantitative analysis of the $2p_\pi$-AOs orbital ribbon for each type of annulene can be used to establish the linking number, using the protocol described previously.[6] When applied to **1**, this reveals that there are two paths which a $2p_\pi$-AO ribbon can follow (Fig. 2), the divergence occurring at the sp-hybridized digonal carbon (labeled 4 in Fig. 2).

One path (Fig. 2a) results in a two-edged ribbon with $L_k = 0$; the other (Fig. 2b) in a single edged ribbon with $L_k = 1$, comprising contributions of $T_w = 0.96$ and $W_r = 0.04\pi$. This duality is also apparent from inspection of the π-electron density isosurface $\rho(r)_\pi$ of **1** (the visual clarity of the resulting $\rho(r)_\pi$ isosurface was enhanced by also calculating the fully fluorinated analogue of **1**, which has the effect of reducing the mixing of the $2p_\pi$-AOs with the 2σ-AOs in the π-MOs of these systems). The computed $\rho(r)_\pi$ isosurface for **1** does indeed show characteristics of **both** a 1_1 torus knot **and** a 0_2 torus link (Fig. 3 and Table 1). Significantly, the two torus curves are connected by a feature associated with the digonal atom (Fig. 2, atom 4) and which has some of the characteristics of a wormhole. As used in physics, the term relates to a valid topological solution to the general relativistic equations describing (4D) spacetime. The analogy used here is of a worm traveling over the skin of an apple and referring to the shortcut possible for the worm to burrow through the core of the apple rather than traveling the entire distance around.

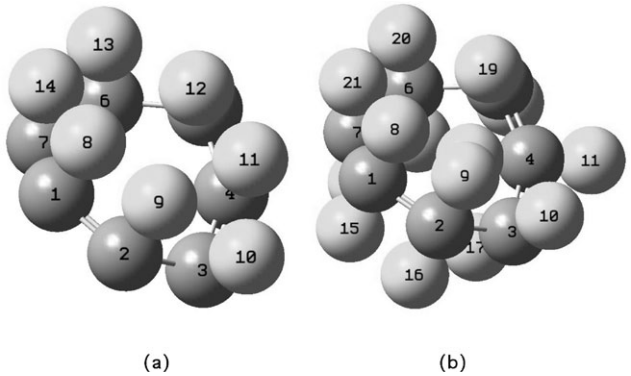

Fig. 2 Two possible ways of constructing a ribbon using the $2p_\pi$-AOs in **1** as vertices. (a) One edge of the ribbon is defined by atoms 1–7; the other by the $2p_\pi$-AO lobes 8–14, including the $2p_\pi$-AO lobe 11 located on the digonal atom 4. Such a ribbon has $L_k = 0.0$. (b) The (single) edge of the ribbon is defined by atoms 1–7, and $2p_\pi$-AO lobes 8–21, with 11 corresponding to the $2p_\pi$-AO on digonal atom 4, orthogonal to that selected for (a). Such a ribbon has $L_k = 1\pi$ ($T_w = 0.96$ and $W_r = 0.04\pi$). The bond angle subtended at atom 4 is 138°. The torsion 10–3–4–11 is 26° (a) and 65° (b). The torsion 2–3–5–6 is 44°.

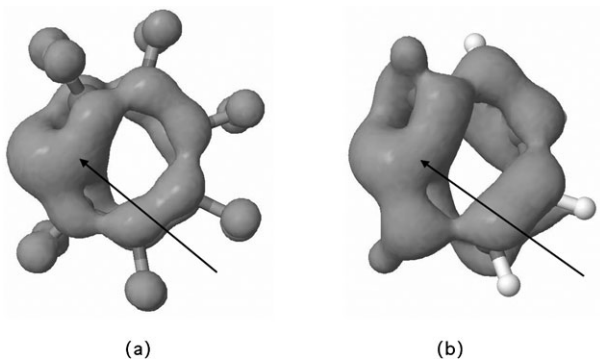

Fig. 3 Electron density $\rho(r)$, evaluated using only the π-like molecular orbitals and contoured at an isosurface of 0.02 a.u. for (a) perfluorinated **1** and (b) hydrogen substituted **1**. The region of the wormholes is indicated with an arrow. Rotatable colour versions of these and all other $\rho(r)$ surfaces can be viewed in the HTML version of this article, *via* Table 1.

Wormhole is used here in a chemical (rather than formal topological) sense to describe the tube or throat connecting two (or more) regions of the $\rho(r)_\pi$ isosurface torus.

The required continuous transformation between a torus link and a torus knot for enantiomerization of **1** *via* **2** now has a simple mechanism. For the transition state **2**, the wormhole or throat is closed. When a C_2-symmetric twist is applied to **2** (following the single imaginary normal transition mode), the wormhole or throat gradually and continuously opens until it reaches the extent visible for **1**. The boundaries of the wormhole persist as the density value of the isosurface increases, until eventually the $\rho(r)_\pi$ torus itself bifurcates into separated basins. In planar **2**, the π-electron density torus need complete only one circuit of the ring to return to its starting position. In a torus knot, as noted above, two such circuits are needed (Fig. 1b). A connecting wormhole or throat connecting the two torus curves means that the density can simultaneously sustain characteristics of both a π-Möbius torus knot and π-Hückel torus link. It should also be noted that this concept of a wormhole is only an approximation in that it relates to the $\rho(r)_\pi$ torus, which is itself an approximation, since π/σ separation can only be achieved based on the energy difference between the two sub-sets of electrons (rather than *via* symmetry-induced orthogonality). Thus the $\rho(r)_\pi$ torus computed for the unfluorinated version of **1**, although similar in its essentials to the fluorinated version, shows further small wormholes connecting the 0_2 and the 1_1 torus curves *via* density on the hydrogen atoms (Table 1), the chemical interpretation of which is not considered further here.

An approximate measure of the nature of the cyclic ring current in terms of its diatropic (aromatic) or paratropic (anti-aromatic) character can be obtained using a NICS (nucleus independent chemical shift)[15] probe placed at a ring centroid and termed NICS(0). More accurate estimates of this character can be obtained by suitable dissections of the NICS tensor components such as $NICS_{zz}$ as well as ring-current densities parallel to the molecular plane arising from a perpendicular magnetic field.[16] However, these methods cannot be easily applied to helical molecules, where no molecular plane is uniquely definable, and the methodology for analyzing ring-current maps for such helical aromatic systems is not yet available. Accordingly, the ring-centroid based NICS(0) was employed here as merely an approximate measure of the nature of the π-ring current, with one modification to the standard procedure of defining the ring centroid based on the nuclear positions of a planar cycle. The modification involves adopting[17] a procedure based instead on the coordinates of the ring-critical point (rcp) derived from an AIM analysis. The difference between NICS(0) and NICS(rcp) was found to be modest.[17]

The computed NICS(rcp) value for perfluorinated **1** (−12.9 ppm) indicates a significantly diatropic and hence aromatic ring current for **1**, an effect which is unlikely to be masked by local effects due to the σ-framework. This suggests that the $4n$-π-Möbius and $4n + 2$-π-Hückel contributions cooperate rather than cancel, their co-existence enabled by the connecting wormhole in the $\rho(r)_\pi$ torus (Fig. 3). Given that the term *double aromaticity*[18] is normally reserved for describing systems with $4n + 2$ Hückel π- and σ-circulations arising from different sub-sets of electrons in orthogonal planes, a term which differentiates the effect described here might be *Janus aromaticity*. This arises from the dual character arising from (predominantly) the same sub-set of electrons having both a $4n + 2$ Hückel and a $4n$ Möbius π-faced topology (and which are not separated by orthogonal planes). This is also subtly different from the recently reported examples of expanded porphyrins with a "split or dual personality," which can switch between two different geometric conformations, one sustaining a paratropic (anti-aromatic) Hückel form and the other a diatropic aromatic Möbius mode.[19]

This wormhole is a feature of both **1** and the twisted azepine **4**, X = F. The latter provides a linking number analysis of $L_k = 1$, $T_w = 0.99$, $W_r = 0.01\pi$ for the torus knot ribbon, but it differs in one significant regard from **1**. The N–X bond is already occupied by a σ-electron pair, and hence it cannot sequester any more electrons. As a result, both the electron density torus knot and the link are associated with a

Table 1 Wormholes in chemical space connecting torus knot and torus link electron density topologies. Full table functionality available in online version

System, symmetry			Wormhole connection	Digital OAI repository[18]
Δ_r[a]	$\rho(r)_\pi$[b]	NICS(rcp)[c]		
1, C_2			1_1 Torus knot +	10042/to-811
0.046	rho(r) rho(r) H[d]	-12.9	0_2 Torus Link	10042/to-815
4, X=F, C_2			1_1 Torus knot +	10042/to-800
0.108	rho(r)	-6.5	0_2 Torus Link	10042/to-816
4, X=Cl, C_2			1_1 Torus knot +	10042/to-801
0.093	rho(r)	-1.8	0_2 Torus Link	
4, X=Br, C_2			1_1 Torus knot +	10042/to-802
0.096	rho(r)	-0.8	0_2 Torus Link	
5, C_2			1_1 Torus knot +	10042/to-822
0.069	rho(r)	-10.1	0_2 Torus Link	
6, C_2			1_1 Torus knot +	10042/to-812
0.052	rho(r)	-11.7	0_2 Torus Link	10042/to-818
7, C_2			1_1 Torus knot +	10042/to-809
0.122	rho(r)	-3.9	2_2 Torus Link	
8, X=F, C_2			1_1 Torus knot +	10042/to-808
0.065	rho(r)	-3.2	0_2 Torus Link	10042/to-817
8, X=Cl, C_2			1_1 Torus knot +	10042/to-813
0.046	rho(r)	-4.3	0_2 Torus Link	
8, X=Br, C_2			1_1 Torus knot +	10042/to-814
0.047	rho(r)	-2.7	0_2 Torus Link	
9, C_2			1_1 Torus knot +	10042/to-810
0.015	rho(r)	-10.0	0_2 Torus Link	
11, X=F, C_2			1_1 Torus knot +	10042/to-826
0.103	rho(r)	-4.6	2_2 Torus Link	
11, X=Cl, C_2			1_1 Torus knot +	10042/to-827
0.101	rho(r)	-3.0	2_2 Torus Link	

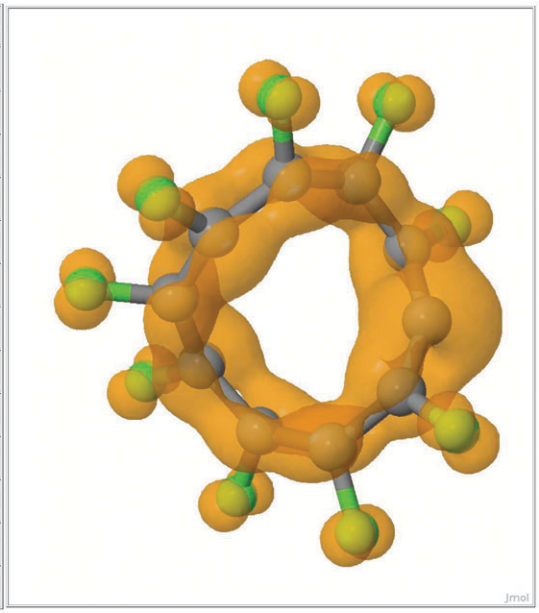

[a] Maximum difference in C–C bond length (Å), not including C═C═C distances. [b] Electron density function evaluated using only ~π molecular orbitals, and contoured at 0.02 a.u. [c] Nucleus independent chemical shift, evaluated at the position of the ring centroid obtained from an AIM analysis of $\rho(r)$. [d] Evaluated for ring fully substituted with H; all other systems are fully substituted with F.

$4n$-π-electron count. Whilst the former favours diatropic character/aromaticity, the latter favors paratropic character/anti-aromaticity. Unlike **1** therefore, the contributions from the two wormhole-connected torus curves partially cancel rather than coincide. The degree of cancellation, and the size of the associated wormhole is however quite sensitive to the *N*-substitution. Progressing from X = F to X = Cl and X = Br, the wormhole shrinks (Table 1), and the torus increasingly loses its knot character and the Möbius-aromatic component associated with this topology. The outcome is that the system tends towards the non-aromaticity associated with a non-planar Hückel anti-aromatic molecule (such as cyclo-octatetraene).

Replacing the azepine nitrogen with an oxepine (as in **5**) induces yet another variation. Whereas the wormhole was located in the region of the heteroatom for **4**, the geometry of **5** undergoes a barrierless rearrangement to sustain instead a *trans* conformation at C3–C4.[14] The resulting $\rho(r)_\pi$ torus takes the form of a knot, but no prominent wormhole is apparent at the heteroatom, or indeed elsewhere. Since $\rho(r)_\pi$ has no torus link character, there is no $4n$ Hückel anti-aromatic contamination and this ring now constitutes an almost pure Möbius-aromatic system (NICS(rcp) −10.1 ppm) with no Janus character. This raises the intriguing possibility that the presence and location of wormholes of this type might be susceptible to rational design with appropriate geometries and substituents.

12-π/10-π-systems

Given this sensitivity of the wormhole to substituent and structure, further structural variation was explored by homologating **1** from an 8-π to a 12 π-electron system. The anionic **6** is a 10-membered ring homologue for which $L_k = 1$, $T_w = 1.08$, $W_r = -0.08\pi$ and it exhibits the same prominent wormhole as **1** (Table 1). The planar form of **6** can sequester an electron pair into the σ-system (again as a carbene), which renders the remaining π-electrons $4n + 2$ aromatic. The resulting Janus-behavior is as described above for **1**, with both torus forms sustaining a diatropic NMR ring current and the outcome being a value NICS(rcp) of −11.7 ppm congruent with aromaticity.

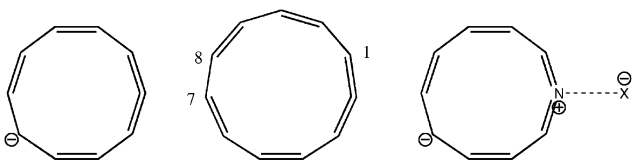

6 **7** **8**

The larger 11-membered ring homologue **7** now accumulates too much angular strain, and this is relieved by a barrierless *trans*-twist distortion in the region of the C7–C8 bond which contributes a further half-twist to the topology (*i.e.* increments L_k by π). The $\rho(r)_\pi$ torus now shows new features, manifesting as a 2_2 torus link connected by a wormhole to a 1_1 torus knot (*cf.* Fig. 1b and c and Fig. 4).

Linking number analysis for the two possible orbital ribbons reveals $L_k = 2$, $T_w = 1.58$, $W_r = 0.42$ and $L_k = 1$, $T_w = 0.58$, $W_r = 0.42\pi$ respectively (the value of W_r is common since they both share the same central curve[6]). Both the torus curves derive from $4n$ π-electrons, and whilst $L_k = 1$ implies aromaticity for such an electron count, $L_k = 2$ in turn implies anti-aromaticity.[4,6] The outcome, as measured using a

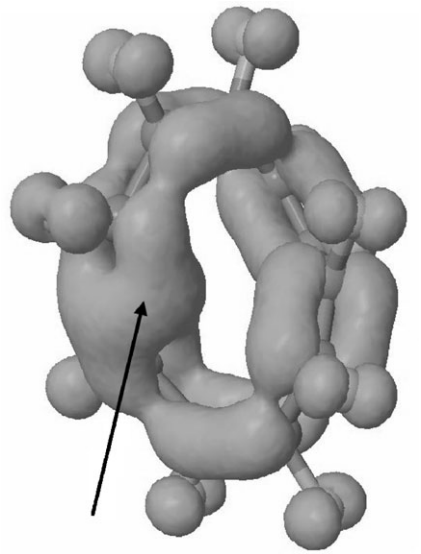

Fig. 4 Electron density $\rho(r)$, evaluated using only the π-like molecular orbitals and contoured at an isosurface of 0.015 a.u. for (perfluorinated) **7**. The region of the wormhole is indicated with an arrow.

NICS(rcp) probe is that the aromaticity and anti-aromaticity largely cancel, a reprise of the situation for **4**. The overall effect is one of merely mild or non-aromaticity.

for the inter-conversion of two enantiomers of a dis-symmetric (chiral) Möbius cycle. The topology of the electron density torus for systems such as **1** reveals the formation of a wormhole or throat connecting the torus link corresponding to Hückel-aromatic behavior and the torus knot corresponding to Möbius-aromaticity. This wormhole allows the molecule to exhibit dual Janus-like aromaticity with both Hückel and Möbius π-electronic properties. The appearance of this wormhole may also be sensitive to the particular geometry and electronic nature of the cycle.

Computational details

Calculations were performed at the B3LYP DFT level and 6-31G(d) basis set level, as implemented in the Gaussian 03 (revision E.01) program.[20] AIM critical points, and the molecular graphs that map their connectivity were obtained by exporting a WFN file from Gaussian and importing into AIM2000.[21] The ring critical point coordinates so obtained were used to evaluate the NICS (rcp) values using Gaussian 03 and the GIAO NMR method.[15] $\rho(r)_\pi$ cubes were calculated using Dgrid[22] fed by an FCHK file exported from Gaussian, and then converted to an isosurface expressed as a JVXL file for visualization using Jmol as presented in Table 1. These files and coordinates are all available *via* the digital repository entries[23] listed in Table 1.

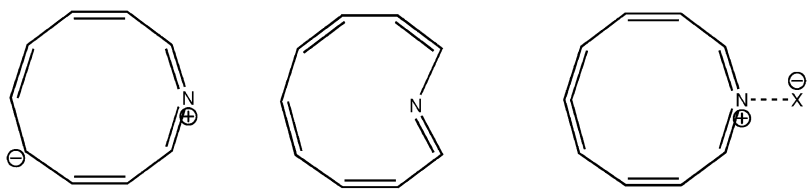

9 **10** **11**

The homologated azepine studied was **8**, for which a wormhole linking a 1_1 torus knot to a 0_2 torus link is now prominent for the entire series X = F, Cl and Br (Table 1). Like **4** and **7**, the overall systems are not strongly aromatic because of the mutual cancellation of 4*n* Möbius aromaticity and Hückel anti-aromaticity. The fully ionized system **9** differs; freed from the restraint of the halogen counter-ion, the planar Hückel form can now sequester an electron pair into an inward facing position (**10**) and again we see Janus–Hückel–Möbius aromaticity.

The final example **11**, X = F combines the characteristics of **1**, **4** and **7**. Two wormholes, a small one at the nitrogen, and a large one at the central allene carbon now connect a 2_2 with a 1_1 torus. As before, the Janus effect results in the Hückel and Möbius aromaticities opposing, resulting in overall non-aromaticity.

Conclusions

A simple topological mechanism is presented for how a Hückel planar π-annulene can be a formal transition state

References

1 *Möbius and his Band*, ed. J. Fauvel, R. Flodd and R. Wilson, Oxford University Press, Oxford, 1993, pp. 122; C. Pickover, *The Möbius Strip*, Thunder's Mouth Press, New York, 2006.

2 E. Heilbronner, *Tetrahedron Lett.*, 1964, 1923–1928, DOI: 10.1016/S0040-4039(01)89474-0.

3 H. S. Rzepa, *Chem. Rev.*, 2005, **105**, 3697–3715, DOI: 10.1021/cr030092l; R. Herges, *Chem. Rev.*, 2006, **106**, 4820–4842, DOI: 10.1021/cr0505425; D. Ajami, K. Hess, F. Koehler, C. Naether, O. Oeckler, A. Simon, C. Yamamoto, Y. Okamoto and R. Herges, *Chem.–Eur. J.*, 2006, **12**, 5434–5445, DOI: 10.1002/chem.200600215 and references cited therein.

4 H. S. Rzepa, *Org. Lett.*, 2005, **7**, 4637–4639, DOI: 10.1021/ol0518333; H. S. Rzepa, *Org. Lett.*, 2008, **10**, 949–952, DOI: 10.1021/ol703129z.

5 R. P. John, M. Park, D. Moon, K. Lee, S. Hong, Y. Zou, C. S. Hong and M. S. Lah, *J. Am. Chem. Soc.*, 2007, **129**, 14142–14143, DOI: 10.1021/ja075945w. For a linking number analysis of this system, see: H. S. Rzepa, *Inorg. Chem.*, 2008, **47**, 8932–34, DOI: 10.1021/ic800987f.

6 S. M. Rappaport and H. S. Rzepa, *J. Am. Chem. Soc.*, 2008, **130**, 7613–7619, DOI: 10.1021/ja710438j.

7 C. S. Wannere, C. Rinderspacher, A. Paul, H. S. Rzepa, H. F. Schaefer, P. v. R. Schleyer and S. M. Allan, *Chem.–Eur. J.*, 2008, submitted for publication.

8 A. V. Chernavskii, in *Linking Coefficient*, ed. M. Hazewinkel, Encyclopaedia of Mathematics, Kluwer Academic Publishers, 2001.

9 For a discussion of the relationship between the chirality of a torus knot and its enantiomers, see: G. H. Wagniere, *J. Math. Chem.*, 2007, **41**, 27–41, DOI: 10.1007/s10910-006-9086-9.

10 For a recent discussion of chiral connectedness, see P. W. Fowler, *Symmetry Culture and Science*, 2005, **16**, 321–334, and references cited therein; A. B. Buda and K. Mislow, *J. Am. Chem. Soc.*, 1992, **114**, 6006–12, DOI: 10.1021/ja00041a016.

11 This point is further elaborated in J. Berson, *Chemical Creativity. Ideas from the Work of Woodward, Huckel, Meerwein and Others*, Wiley, New York, 1999.

12 S. Martin-Santamaria and H. S. Rzepa, *Chem. Commun.*, 2000, 1503–1504, DOI: 10.1039/b002922j; S. Martin-Santamaria and H. S. Rzepa, *J. Chem. Soc., Perkin Trans. 2*, 2000, 2372–2377, DOI: 10.1039/b005560n.

13 E. V. Patterson and R. J. McMahon, *J. Org. Chem.*, 1997, **62**, 4398–4405, DOI: 10.1021/jo9613848; M. W. Wong and C. Wentrup, *J. Org. Chem.*, 1996, **61**, 7022–7029, DOI: 10.1021/jo960806a; P. R. Schreiner, W. L. Karney, P. v. R. Schleyer, W. T. Borden, T. P. Hamilton and H. F. Schaefer, *J. Org. Chem.*, 1996, **61**, 7030–7039, DOI: 10.1021/jo960884y.

14 W. L. Karney, C. J. Kastrup, S. P. Oldfield and H. S. Rzepa, *J. Chem. Soc., Perkin Trans. 2*, 2002, 388–392, DOI: 10.1039/b111369k.

15 Schleyer, v. R. Paul, Maerker, Christoph, Dransfeld, Alk, Jiao, Haijun, van Eikema Hommes and J. R. Nicolaas, *J. Am. Chem. Soc.*, 1996, **118**, 6317–6318, DOI: 10.1021/ja960582d; Z. Chen, C. S. Wannere, C. Corminboeuf, R. Puchta and P. v. R. Schleyer, *Chem. Rev.*, 2005, **105**, 3842–3888, DOI: 10.1021/cr030088+. For a comparisonof NICS with a range of other aromaticity indices, see: P. Bultinck, *Faraday Discuss.*, 2007, **135**, 347–365, DOI: 10.1039/b609640a.

16 E. Steiner and P. W. Fowler, *Chem. Commun.*, 2001, 2220. For a recent review of the ipsocentric approach to the calculation of current densities, see: P. W. Fowler, Molecular currents and aromaticity, *AIP Conf. Proc.*, 2007, **963**, 47–53, DOI: 10.1063/1.2827030.

17 C. S. M. Allan and H. S. Rzepa, *J. Org. Chem.*, 2008, **73**, 6615–6622, DOI: 10.1021/jo801022b.

18 J. Chandrasekhar, E. Jemmis and P. v. R. Schleyer, *Tetrahedron Lett.*, 1979, 3707–3710, DOI: 10.1016/S0040-4039(01)95503-0.

19 M. Stepien, L. Latos-Grazynski, N. Sprutta, P. Chwalisz and L. Szterenberg, *Angew. Chem., Int. Ed.*, 2007, **46**, 7869–7873, DOI: 10.1002/anie.200700555; E. Pacholska-Dudziak, J. Skonieczny, J. Pawlicki, M. L. Szterenberg, Z. Ciunik and L. Latos-Grazynski, *J. Am. Chem. Soc.*, 2008, **130**, 6182–6195, DOI: 10.1021/ja711039c.

20 M. J. Frisch, G. W. Trucks, H. B. Schlegel, G. E. Scuseria, M. A. Robb, J. R. Cheeseman, J. A. Montgomery Jr, T. Vreven, K. N. Kudin, J. C. Burant, J. M. Millam, S. S. Iyengar, J. Tomasi, V. Barone, B. Mennucci, M. Cossi, G. Scalmani, N. Rega, G. A. Petersson, H. Nakatsuji, M. Hada, M. Ehara, K. Toyota, R. Fukuda, J. Hasegawa, M. Ishida, T. Nakajima, Y. Honda, O. Kitao, H. Nakai, M. Klene, X. Li, J. E. Knox, H. P. Hratchian, J. B. Cross, V. Bakken, C. Adamo, J. Jaramillo, R. Gomperts, R. E. Stratmann, O. Yazyev, A. J. Austin, R. Cammi, C. Pomelli, J. W. Ochterski, P. Y. Ayala, K. Morokuma, G. A. Voth, P. Salvador, J. J. Dannenberg, V. G. Zakrzewski, S. Dapprich, A. D. Daniels, M. C. Strain, O. Farkas, D. K. Malick, A. D. Rabuck, K. Raghavachari, J. B. Foresman, J. V. Ortiz, Q. Cui, A. G. Baboul, S. Clifford, J. Cioslowski, B. B. Stefanov, G. Liu, A. Liashenko, P. Piskorz, I. Komaromi, R. L. Martin, D. J. Fox, T. Keith, M. A. Al-Laham, C. Y. Peng, A. Nanayakkara, M. Challacombe, P. M. W. Gill, B. Johnson, W. Chen, M. W. Wong, C. Gonzalez and J. A. Pople, *GAUSSIAN 03 (Revision E.01)*, Gaussian, Inc., Wallingford, CT, 2004.

21 F. W. Biegler-König and K. Schönbohm, *AIM2000*. The program can be downloaded at http://www.aim2000.de/.

22 M. Kohout, *DGrid*, version 4.3, 2008.

23 H. S. Rzepa, J. Downing, A. Tonge, F. Cotterill, M. J. Harvey, P. Murray-Rust, P. Morgan and N. Day, *J. Chem. Inf. Model.*, 2008, **48**, 1571–1581, DOI: 10.1021/ci7004737.